

Pre print

GLO13Q1

being reviewed
~~not for pub. dist~~

A Vertical Ground-water Movement Correction for Heat Flow

Arthur J. Mansure and Marshall Reiter

New Mexico Bureau of Mines and Mineral Resources
New Mexico Institute of Mining and Technology

Socorro, N. M. 87801

Abstract

In the presence of forced convection, there exists an energy flux $c\rho\bar{v}T$, because of mass-transported heat energy. By plotting temperature gradient vs. temperature, it is possible to use temperature data to determine the significance of convective heat transfer. Such a plot can be useful even when the flow system is not one dimensional or vertical. As an example of convective heat transfer, a temperature log from the Rio Puerco area of New Mexico shows that downward ground-water movement of 4.7×10^{-7} cm/sec over a 77m interval can reduce the observed geothermal gradient and heat flow by a factor of 2. Such strong perturbations of heat flow by ground water indicate the need for deep heat-flow measurements. Consideration of the convective flux allows one to use total energy balance at the boundary of an aquifer and semiconfining media to obtain hydrological information about the semiconfining layer.

Introduction

Vertical ground-water movement may significantly influence the heat flux reaching the earth's surface [Van Orstrand, 1934]. In order to obtain accurate measurements of the near-surface conductive heat flux, considerable care in analyzing temperature logs is necessary so that zones of ground-water movement may be recognized. Increased uncertainties in conductive heat flow are associated with sites where water movement is indicated on the temperature logs [Reiter et al., p. 813, 1975]. In this paper calculations of heat flow are made that include effects of vertical ground-water movement. It is always desirable to make measurements deep enough to have a high level of confidence that the log has a representative linear-gradient zone below any water movement; however, water movement at a greater depth is always a possibility and may be undetectably changing the heat flux within the logged zone.

Bredehoef and Papadopulos [1965] presented an expression describing the subsurface temperature changes produced within a zone of uniform vertical forced-convective ground-water movement. We will demonstrate how this expression can be applied to subsurface temperature logs exhibiting vertical ground-water movement in order to estimate the heat flux that would occur if there were no ground-water movement.

General Solution to Problem

The steady-state differential equation for an isotropic homogeneous permeable media with simultaneous heat flow and incompressible fluid flow is [de Vries 1958; Stallman, 1963]

$$\nabla \cdot (k \nabla T) - \nabla \cdot (c \rho \bar{V} T) = 0, \quad (1)$$

where T = temperature,

c = heat capacity per unit mass of fluid,

ρ = density of fluid,

k = thermal conductivity of solid-fluid complex, and

\bar{V} = specific discharge of fluid.

The fluid must obey the steady-state continuity equation

$$\nabla \cdot (\rho \bar{V}) = 0,$$

and thus (1) simplifies to

$$\nabla \cdot (k \nabla T) - c \rho \bar{V} \cdot \nabla T = 0. \quad (2)$$

Vertical geothermal gradients are generally much larger than horizontal temperature gradients, suggesting

$$V_z \frac{\partial T}{\partial z} \gg V_x \frac{\partial T}{\partial x} \text{ or } V_y \frac{\partial T}{\partial y}.$$

As such, assuming k is constant,

$$\frac{d^2 T}{dz^2} - \frac{c \rho}{k} \frac{dT}{dz} = 0, \quad (3)$$

where z is the vertical coordinate. This is the one-dimensional

equation considered by Bredehoef and Papadopoulos [1965] . It applies to regionally constant forced-convective water movement in the vertical direction (Figure 1). Bredehoef and Papadopoulos [1965] obtained a solution to (3) by referring to temperatures T_0 and T_L (Figure 1), the upper and lower temperatures of a zone of length L within which the specific discharge is a constant. Their solution is

$$T = (T_L - T_0) \left\{ \exp(\beta z/L) - 1 \right\} / \left\{ \exp(\beta) - 1 \right\} + T_0, \quad (4)$$

where T is the temperature at point z , z is the distance down from T_0 , and $\beta = c\rho V_z L/k$ (a dimensionless parameter that is positive or negative depending on whether V_z is downward or upward, respectively). T_0 and T_L do not need to correspond to the top or bottom of the media under investigation and may be any convenient pair of experimentally measured points within this media.

The customary method of determining terrestrial heat flow is to multiply temperature gradients obtained from logs with the rock conductivities measured in the lab, i. e.,

$$Q = -k \frac{dT}{dz} . \quad (5)$$

In the presence of fluid movement the total energy flux includes an "internal heat energy" carried by the mass movement of fluid, as well as conduction [de Vries, 1958; Lubimova et al., 1965] .

This total energy flux is

$$E = -k \frac{dT}{dz} + \rho c_p V_z (T - T'), \quad (6)$$

where T' is the temperature at which the "internal heat energy" is taken to be zero. The importance of using total energy flux can be demonstrated by differentiating (4)

$$\frac{dT}{dz} = (\beta/L) (T_L - T_0) \exp(\beta z/L) / \{ \exp(\beta) - 1 \}. \quad (7)$$

This gradient is not a constant (it is a function of position) and hence cannot be used with Fourier's heat conduction equation (5), because the principle of conservation of energy would be violated. However, if (4) and (7) are substituted into (6), the result is

$$E = - \frac{\beta k}{L} \left\{ \frac{T_L - T_0}{\exp(\beta) - 1} - (T_0 - T') \right\}. \quad (8)$$

This expression is independent of the position z within the zone of uniform ground-water movement; therefore, conservation of energy is maintained. In the limit $V_z \rightarrow 0$, this total energy flux expression reduces to $-k(T_L - T_0)/L$, the appropriate energy flux for conduction. E , rather than Q , is the energy flux to use in regions of constant vertical forced convection. Henceforth we shall refer to E as the "heat flow."

With total energy-flux expression (6), we can interpret the temperature vs. depth profile described by (4). When water is moving downward ($\beta > 0$), the temperature vs. depth profile is as shown on Figure 2. If there were no water movement (heat transported by conduction only), we would expect to see the straight dotted line from T_0 to T_L . When water of a given temperature is moving downward, we must go deeper than if there was no water movement to encounter the same temperature (vertical line on Figure 2); or at a fixed depth the observed temperature is less than if there were no ground-water movement (horizontal line on Figure 2). The profile is a curved rather than a straight line because the amount of heat being carried back downward by forced convection is not constant but is changing with depth. The amount of mass-transported energy changes because the ability of water to transport energy by convection is proportional to the absolute temperature, which of course changes with depth, c.f. second term (6).

Application of Theory to Field Data

As an example of heat flux including convection, we shall consider the Rio Puerco #1 log shown in Figure 3. Between 60m and 100m the temperature vs. depth profile in Figure 3 appears linear, and, hence, it is reasonable to assume no effects of ground-water movement within this zone. In this region the data fits a straight line with an accuracy $\pm 0.002^\circ\text{C}$ (see Table 1), the limit of the precision of our platinum sonde--Mueller bridge measuring system.

Between 120m and 180m the gradient shown in Figure 3 systematically curves with deviations from a straight line 30 times the precision of the measuring system. Assuming a constant thermal conductivity, the changing gradient between 120m and 180m implies Fourier's law will not give consistent heat flow. Before we may assume vertical water movement and apply (6) or (8), we must be sure that the actual curvature is that prescribed by (4). A test of the appropriateness of (6) or (8), the equations for the total heat flow, is then how well the experimental data fits (4), the equation describing the temperature in the presence of forced, vertical convection.

Region III has experimentally significant nonlinearities; however, with only three data points it is not possible to tell if the nonlinearities are systematic or random. Conclusions about water movement in Region III cannot be made at this time.

It is possible to analyze experimental data directly by curve fitting to (4). However, because of statistical problems and experimental errors, it is more advantageous to analyze the character of data exhibiting potential vertical ground-water flow by plotting $\Delta T/\Delta z$ vs. T . This plot can be understood by rearranging (6) to obtain

$$\frac{dT}{dz} = (\beta/L)(T - T') - E/k, \quad (9)$$

a linear equation of the variable T . Thus, plots of $\Delta T/\Delta z$

vs. T yield straight lines when β is constant. Regions of no water movement ($\beta = 0$) yield horizontal lines on such a plot. Regions of uniform forced, vertical convection ($\beta \neq 0$; $\beta = \text{constant}$) yield nonhorizontal lines.

Figure 4 is a $\Delta T/\Delta z$ vs. T plot for the experimental data of the Rio Puerco #1 log. There are three different zones representing separate temperature vs. depth characteristics. Region I is characterized as nearly horizontal in agreement with the linear fit of temperature vs. depth noted in Table 1 and in agreement with the hypothesis of no vertical water movement. Region II has a non-zero slope and fits a linear line that is indicative of uniform water movement. The points of Region III are almost horizontal, probably indicating little vertical ground-water movement.

From Figure 4 we can determine the parameters (slope and intercept) of (9), i.e.,

$$\beta/L = .00862 /m , \quad (10)$$

and (11)

$$- E/k = - .114 \text{ } ^\circ\text{C}/m ,$$

for Region II of the Rio Puerco #1 log (T' taken to be 0°C). Since (4) does not contain E , in order to use (10) and (11) to determine the amount of vertical ground-water movement, we rearrange (8) to give

$$\frac{T_L - T_0}{\exp(\beta) - 1} = -(E/k)/(\beta/L) + T_0 , \quad (12)$$

which substituted into (4) yields

$$T = \left\{ -(E/k)/(\beta/L) + T_0 \right\} \left\{ \exp(\beta z/L) - 1 \right\} + T_0 . \quad (13)$$

To use (13) to describe the temperature of Région II we still need T_0 , the temperature at the depth where z is taken to be zero. At this point we have a choice. T_0 can be taken to be one of the experimentally measured temperatures, or we may consider it a parameter that is varied until (13) most accurately describes the data of Region II. Measuring z from 160m, we found that the best T_0 is $.004^\circ\text{C}$ higher than the temperature 19.772°C measured at this point (this is within the experimental error of the measurement). With this choice of $T_0 = 19.776$, (13) becomes

$$T = 6.53^\circ\text{C} \left\{ \exp(.00862 z) - 1 \right\} + 19.776^\circ\text{C} , \quad (14)$$

which gives the fit shown in Table 2. The table shows that the depth vs. temperature relationship of Bredhoeft and Papadopulos [1965], (4), describes the observed temperatures of Region II of the Rio Puerco #1 log much better than the linear fit tried in Table 1. In fact, the average deviation of data points in Region II, assuming uniform forced convection ($.004^\circ\text{C}$), is not significantly different than the average deviation of data points in Region I, assuming no water movement, and probably represents the experimental error. Thus,

we can as reasonably assume uniform forced convection in Region II as we can assume no water movement in Region I. Table 2 also shows that poor fits are obtained to the data if the forced convection of Region II is assumed to continue into Regions I and III. This poor fit is as expected from Figure 4 and supports our earlier supposition that Regions I, II, and III represent separate hydrothermal conditions. Region III does not give a good fit in either Table 1 or 2. Comparing the tables and figures, it is most likely there is no water movement in Region III; however, the statistics are not conclusive.

Heat Flow

If there is no vertical water movement in Regions I and III, then water must come to the area at the boundary of Regions I and II and leave the area at the boundary of Regions II and III. Figure 5 shows the overall energy balance, including the energy transported by the assumed water movement at the boundaries between the regions.

With the linear fits of Table 1 along with (10) and (11), Q_1 , E_1 , E , E_2 , and Q_2 can be calculated to determine if the vertical energy flow is consistent. A better test of continuity of energy was derived by Negi and Narain Singh [1967].

They found

$$Q_2/Q_1 = \exp(\beta). \quad (15)$$

Their derivation used only the continuity of temperature gradients for boundary conditions, rather than the energy relations of Figure 5; however, the energy boundary conditions of Figure 5 together with (4) and (7) can also be shown to yield (15).

Since we already know β/L from (10), all we need to apply equation (15) is the total distance over which the water is moving down. This distance can be found by locating the boundaries of the regions by simultaneously solving (14) with the linear fits to the temperatures of Regions I and III. Our best estimate of these boundaries is 113m and 190m. Thus our analysis of Region II, based on the assumption of uniform forced convection in this region, predicts

$$Q_2/Q_1 = \exp\{0.00862(190 - 113)\} = 1.94 \quad (16)$$

This can be compared to

$$Q_2/Q_1 = k \cdot 0.0742 / k \cdot 0.0369 = 2.01, \quad (17)$$

based on the fitted gradients of Regions I and III. This agreement is quite good considering the uncertainties about Region III and the assumption of equal conductivities in all three regions. Equation (15) also shows that heat flow measured above and below a semiconfining layer may give information about the hydrological conditions (β) that exist

within the semiconfining layer even when no data are available from within the layer itself.

The primary uncertainty in the calculation of (16) is the effect that the uncertainty of the true gradient in Region III has on the calculation of the boundary at 190m. Inspection of Figure 4 shows that this boundary should not be wrong by more than 5m. Such an error would cause a 5% error in calculating the ratio Q_2/Q_1 .

Water Movement within the Wellbore

In order to accept the heat flow analysis in the last section, we must address the problem of fluid movement within the formation vs. fluid movement within the wellbore. Temperature disturbances due to fluid movement within wellbores have received considerable attention in petroleum technology. In particular, Ramey [1962] found a relation that approximates the temperature in a well where fluids are moving

$$T = T_0 + gz + \{ \exp(-z/A) - 1 \} Ag, \quad (18)$$

where T is the observed temperature, T_0 is the temperature at the point of fluid entry into the wellbore, z is the distance from T_0 , g is the normal geothermal gradient, and A is a measure of the rate of heat transfer between the moving fluid and the formation surrounding the wellbore.

In (18) the presence of the linear z dependent term (second term on RHS) means that the depth vs. temperature profile for fluid moving in the wellbore is different from the depth vs. temperature profile found by Bredehoeft and Papadopoulos [1965] for uniform vertical water movement in the formation. Hence, (18) will not give a straight line on a plot of $\Delta T / \Delta z$ vs. T .

Temperature vs. depth profiles, as given by (18), are shown in Figure 6 for an undisturbed geothermal gradient of $20^{\circ}\text{C}/\text{km}$. The solid line shows the natural geothermal profile. At 100m water enters the wellbore and moves down to 200m. The dotted line, marked $A = \infty$, shows the profile observed when the water moves down so rapidly that it is not able to absorb a significant amount of heat from the formation. The solid line, marked $A = 0$, shows the profile observed when the water moves down so slowly it is always in equilibrium with the surrounding formation. The curve, marked $A = 50\text{m}$, represents an intermediate flow rate. The value of 50m was chosen because it gives a curvature that is qualitatively similar to that observed over the 77m depth interval of Region II of the Rio Puerco #1 log.

Ramey [1962] shows that for a 7" diameter well injecting 4,790 barrels of water per day for 75 days, $A = 30,400$ ft. Ramey's expression for A shows that A is proportional to u (the velocity of fluid down the wellbore); therefore, our example of $A = 50\text{m}$ implies

$$\begin{aligned}
 u &= \frac{50\text{m}}{30400\text{ft}} \times 4790 \text{ bbl/d @ 7" } \times \frac{30 \text{ ft/min}}{2000 \text{ bbl/d @ 7" }} \\
 &= 2.4 \times 10^6 \text{ in/yr } \quad \text{or} \quad .2 \text{ cm/sec.}
 \end{aligned}
 \tag{19}$$

The velocity of the fluid movement in the formation of Rio Puerco #1 can be found from (10) and the definition of β

$$\begin{aligned} v_3 &= (\beta/L)(k/c\rho) \\ &= 4.7 \times 10^{-7} \text{ cm/sec} \\ &= 5.8 \text{ in/yr,} \end{aligned} \tag{20}$$

using 5.5×10^{-3} cal/cm-sec $^{\circ}$ C for the thermal conductivity. Water moving within the wellbore (18) not only has a different functional dependence of temperature vs. depth than water moving in the formation (4), but also to produce a similar temperature vs. depth profile, it must be almost six orders of magnitude larger. The estimated velocity u for movement within the wellbore is large enough, compared with times over which temperature measurements are made, that one would expect to observe temperature fluctuations due to turbulence during the equilibrium temperature logging procedure [Reiter et al., 1976]. The absence of unusual temperature fluctuations being observed during the logging of Rio Puerco #1 supports the conclusion that Figure 3 is representing fluid moving in the formation and not fluid movement within the wellbore.

Applicability of the Analysis

It is important to consider under what circumstances the preceding one-dimensional analysis is adequate. Domenico and Palciauskas [1973] solved a two-dimensional flow problem. Their results indicate (4) can be considered the first term in the expansion solution of a two-dimensional problem. They

also found that in two dimensions, the ratio of depth to length of the water flow is a measure of the ratio of horizontal temperature gradient to natural geothermal gradient. Steady water flow primarily exchanges heat with the surrounding rock when it flows across rather than parallel to the isotherms. Unless the depth-to-length ratio of the basin confining the flow approaches one, or the flow is not steady state, the assumptions that allowed (2) to be reduced to (3) may be valid (see Figure 2 and 3 of Domenico and Palciauskas [1973]).

In cases where the heat flow is uniform but not parallel to the well (as may happen when the well is deviated), it is possible to solve (3) in a reference frame perpendicular to the isotherms and then transform to the vertical axis. Such a transformation shows that as long as the angle between the heat flow and wellbore is not more than 30° , the errors in calculating V_z or E are less than 10%.

Since sufficient hydraulic information is rarely available to decide if (4) applies, it is important to realize that (6)

and Figure 4 represent the vertical component of the total energy flow and are valid even if the flow is not one dimensional. If Figure 4 is linear there is no horizontal flow or it must be parallel to the isotherms and be causing no observable temperature disturbance. Horizontally flowing sheets of water too thin to measure a temperature profile across should be excluded from this argument. If the $\Delta T / \Delta z$ vs. T plot is not linear, conclusions about vertical water movement cannot be made, since a variety of disturbances such as non-constant V_z , horizontal flow, changing thermal conductivity,

or time-dependent effects could be causing the disturbance. The argument that, if $\Delta T/\Delta z$ vs. T gives a linear plot, the only important flow is vertical corresponds to the familiar argument that if the gradient is constant, there is no fluid movement and the temperatures are in equilibrium.

Thermal conductivity

Most of the Rio Puerco #1 log is in rock clearly identified as Mancos shale, which in this area shows no significant lithological variation on γ -ray logs, electric logs, or in fragment samples. Five distinct fragment samples from within Region II were found to have thermal conductivities ranging from 6.1 to 5.0 mcal/cm-sec^{°C} with an average value of $5.5 \pm .4$ mcal/cm-sec^{°C} [Reiter et al., p. 815, 1975]. For a systematic variation of the rock conductivity in Region II to cause the observed gradient change, the in-situ rock conductivity would have to have varied with depth by a factor of 2. Since the observed conductivity variations appear random with depth and much less than a factor of 2, it is unlikely that any conductivity variation is causing the changing gradient seen in Region II. The location of the well within the Rio Puerco fault system suggests vertical ground-water movement may be expected [Woodward et al., 1975; Reiter et. al., 1978].

Conclusions

Our analysis of the Rio Puerco #1 log shows that downward water movement between 113m and 190m has probably reduced the heat flow from 4.1 HFU observed between 190m and 210m to 2.0 HFU

above 113m. However, it is difficult to have a high degree of confidence in a single heat-flow value in such a tectonically and hydrologically complex area. The Rio Puerco region is extensively faulted, and it is possible that the hydrologic condition proposed here may change at faults only a few km away. Below the depth of the temperature data presented in this log, there are at least five known aquifers. There is no way one can assess the thermal influence of these lower aquifers from temperature data above 210m. To have confidence that the 4.1 HFU observed between 190m and 210m represents a non-hydrological heat flow anomaly, we need to obtain very deep geothermal temperatures below any hydrological disturbances. A better understanding of the relationship between heat flow and hydrology permit the use of heat flow or temperature measurements to obtain hydrologic information [Cartwright, 1970; Sorey, 1971] .

Acknowledgments

The cooperation of Continental Oil personnel is appreciated for supervising the well and providing samples for this study. The work was supported in part by National Science Foundation grant GI32482 and the New Mexico Bureau of Mines and Mineral Resources. Mansure was a post-doctoral fellow supported by the National Science Foundation grant.

REFERENCES

- Bredehoeft, J. D., and I. S. Papadopoulos, Rates of vertical groundwater movement estimated from the earth's thermal profile, Water Resour. Res., 1, 325-328, 1965.
- Cartwright, K., Groundwater discharge in the Illinois Basin as suggested by temperature anomalies, Water Resour. Res., 6, 912-918, 1970.
- deVries, D. A., Simultaneous transfer of heat and moisture in porous media, EOS Trans. AGU, 39, 909-916, 1958.
- Domenico, P. A., and V. V. Palciauskas, Theoretical analysis of forced convective heat transfer in regional groundwater flow, Geol. Soc. Amer. Bull., 84, 3808-3813, 1973.
- Lubimova, E. A., R. P. Von Herzen, and G. B. Udintsev, On heat transfer through the ocean floor, Geophysical Monograph Series, No. 8, ed. W. H. K. Lee, pp. 78-86, AGU, 1965.
- Negi, J. G., and R. Narain Singh, On heat transfer in layered ocean sediments, Earth Planet. Sci. Lett., 2, 335-336, 1967.
- Ramey, H. J., Wellbore heat transmission, J. Pet. Tech., 14, 427-435, 1962.
- Reiter, M., C. L. Edwards, H. Hartman, and C. Weidman, Terrestrial heat flow along the Rio Grande Rift, New Mexico and Southern Colorado, Geol. Soc. Amer. Bull., 86, 811-818, 1975.
- Reiter, M., G. Simmons, M. Chessman, T. England, H. Hartman, and C. Wiedman, Terrestrial heat flow near Datil, New Mexico, Annual Report, pp. 33-37, New Mexico Bureau of Mines and Mineral Resources, 1976.
- Reiter, M., C. Shearer, and C. L. Edwards, Geothermal anomalies along the Rio Grande Rift, New Mexico, Geology, 6, 85-88, 1978.
- Sorey, M. L., Measurement of vertical groundwater velocity from temperature profiles in wells, Water Resour. Res., 7, 963-970, 1971.
- Stallman, R. W., Computation of ground-water velocity from temperature data, U. S. Geol. Surv. Water Supply Paper, 1544-H, 36-46, 1963.
- Van Orstrand, C. E., Temperature gradients, in Problems of Petroleum Geology, pp. 989-1,021, Amer. Ass. Petrol. Geol. Bull., 1934.

Woodward, L. A., J. F. Callender, J. Gries, W. R. Seager,
C. E. Chapin, R. E. Filinski, and W. L. Sheffer,
Tectonic Map of Rio Grande Region from New Mexico-
Colorado Border to Presidio, Texas, New Mexico Geological
Society Guidebook 26, 239-240, 1975.

Table 1. LMS fits to the three regions of Figure 3.

Depth	Temp. (observed)	Temp. (fitted)	Difference (observed-fitted)	Average deviation
Region I				.002
60M	15.628	15.630	-.002	
80M	16.371	16.368	+.003	
100M	17.104	17.106	-.002	
Region II				.075
120M	17.877	17.788	+.089	
140M	18.741	18.825	-.084	
160M	19.772	19.863	-.091	
170M	20.368	20.381	-.013	
180M	21.000	20.900	+.100	
Region III				.022
190M	21.794	21.778	+.016	
200M	22.486	22.519	-.033	
210M	23.277	23.261	+.016	

Table 2. Uniform vertical ground-water fit to temperatures of Region II.

Depth	Temp. (observed)	Temp. (fitted)	Difference (observed-fitted)	Average deviation
Region II				.004
120M	17.877	17.871	+0.006	
140M	18.741	18.742	-0.001	
160M	19.772	19.776	-0.004	
170M	20.368	20.364	+0.004	
180M	21.000	21.005	-0.005	
Region III (according to fit of Region II)				.043
190M	21.794	21.703	+0.091	
200M	22.486	22.465	+0.021	
210M	23.277	23.294	-0.017	
Region I (according to fit of Region II)				.187
100M	17.104	17.139	-0.035	
80M	16.371	16.522	-0.151	
60M	15.628	16.003	-0.375	

Fig. 1. Geometry of vertical ground-water movement.

Fig. 2. Depth vs. temperature profile for downward ground-water movement.

Fig. 3. Rio Puerco #1 temperature log.

Fig. 4. $\Delta T/\Delta z$ vs. T plot for Rio Puerco #1 data.

Fig. 5. Diagram of energy balance.

Fig. 6. Temperature vs. depth profiles for fluid movement downward within the wellbore.

FIGURE 1

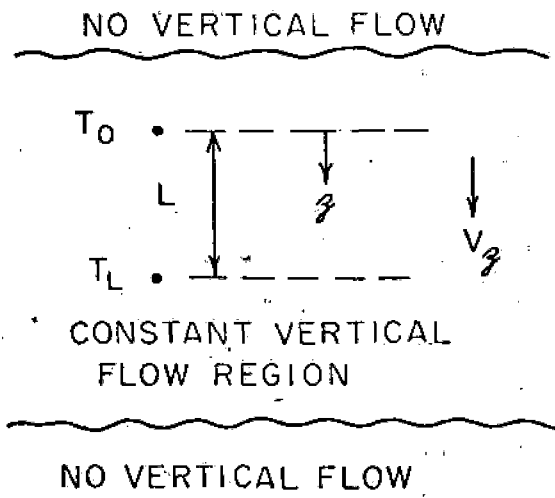
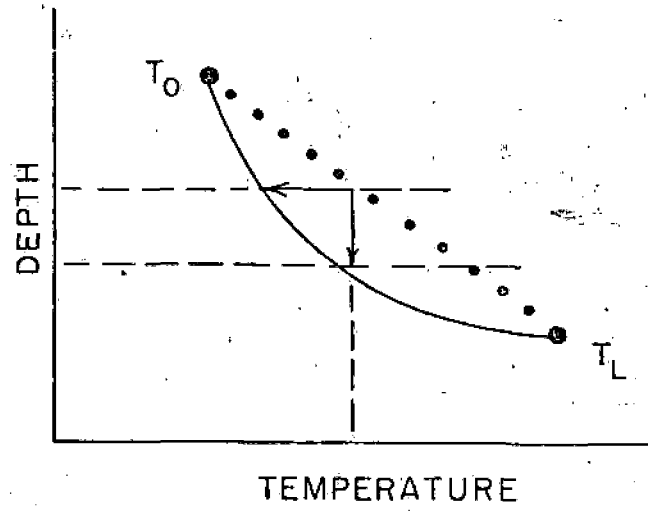


FIGURE 2



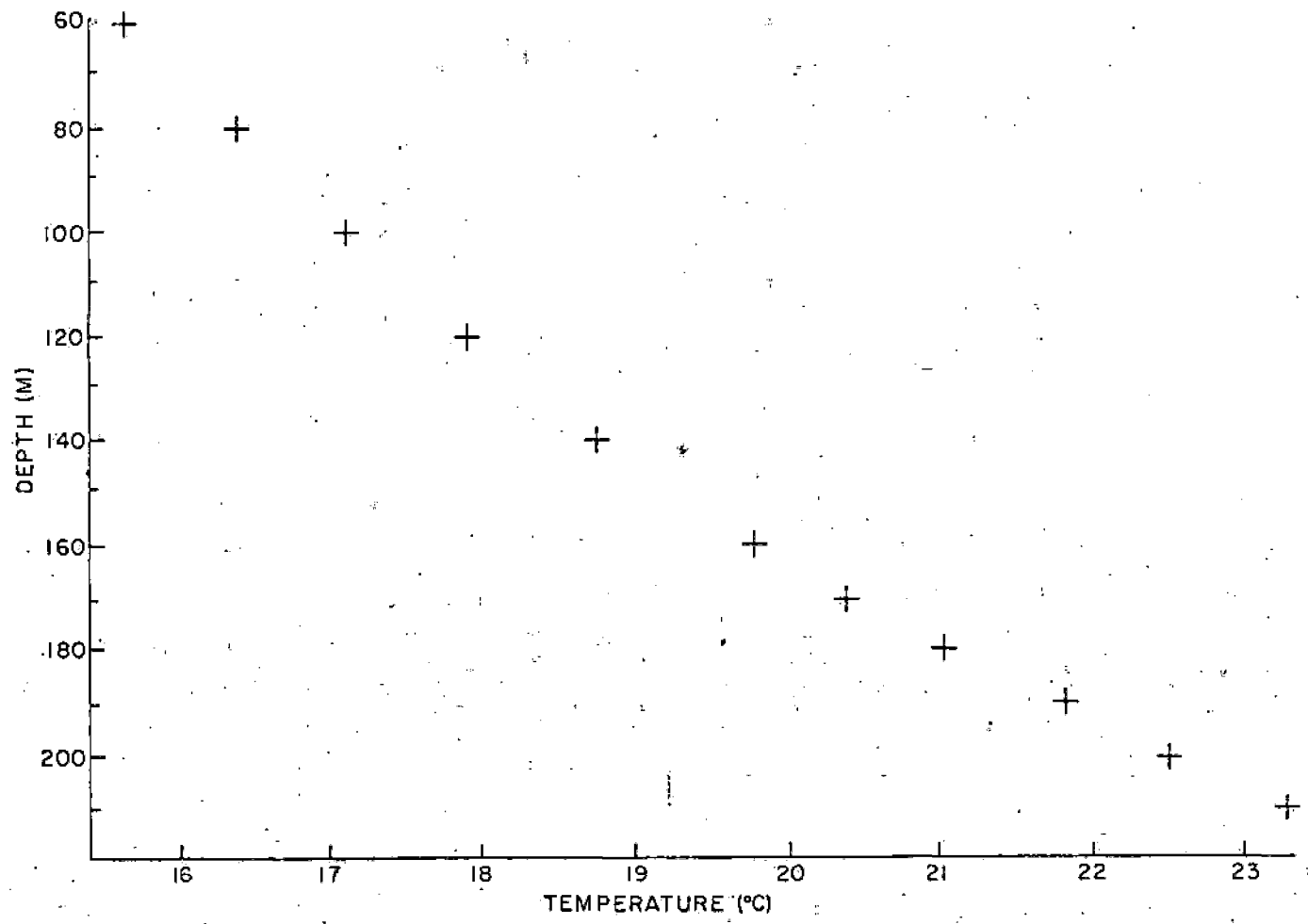


FIGURE 3

FIGURE 4

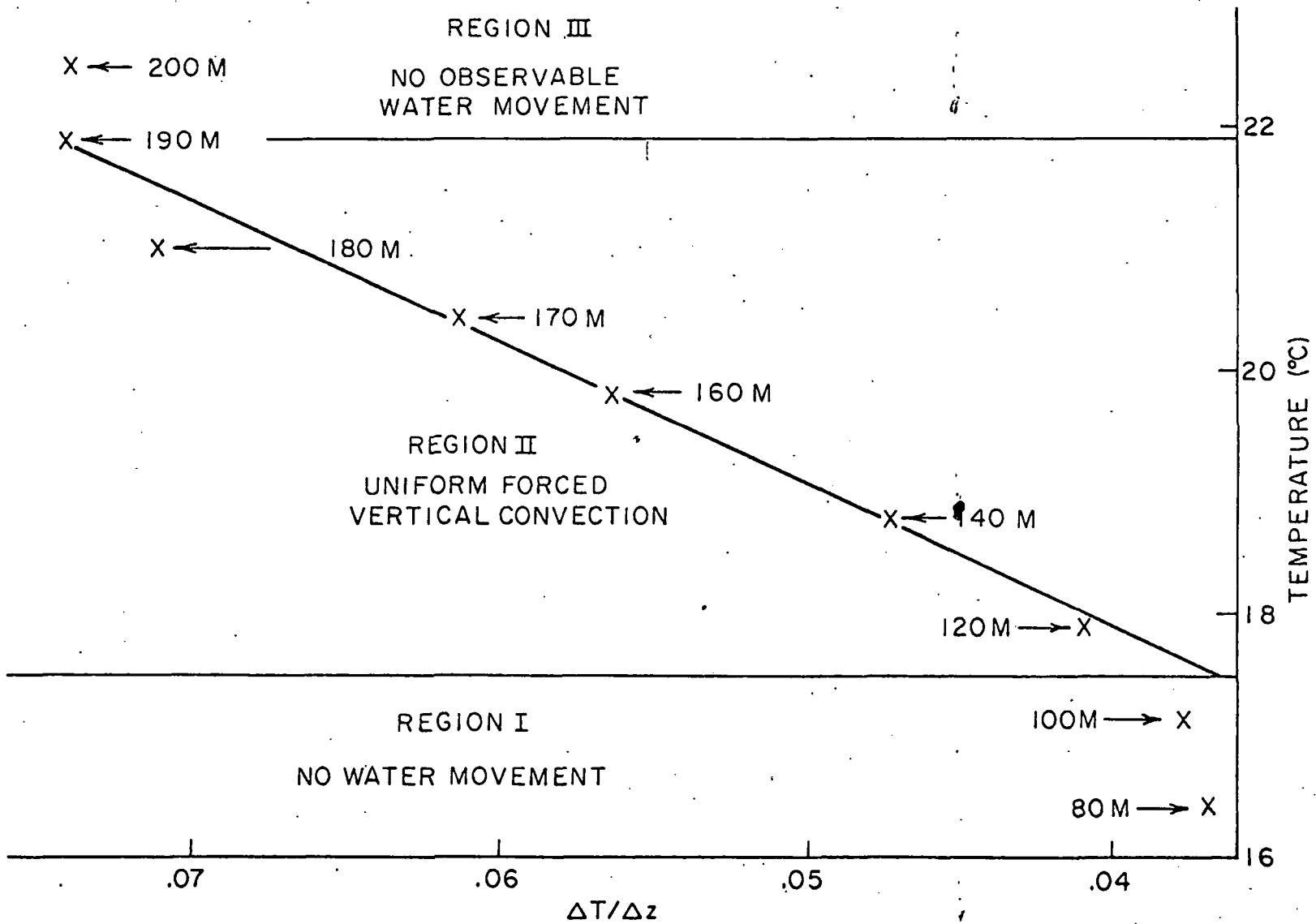


FIGURE 5

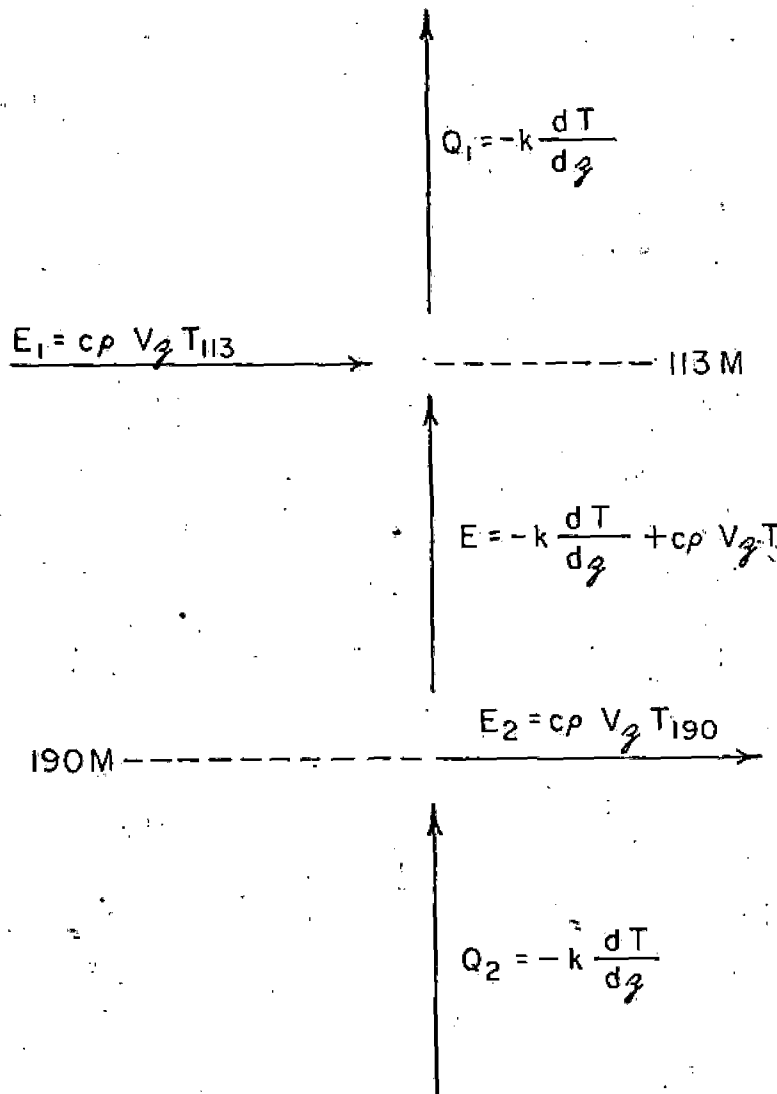


FIGURE 6

